RSC Advances

ROYAL SOCIETY OF CHEMISTRY

www.rsc.org/advances

Cite this: DOI: 10.1039/c0xx00000x

www.rsc.org/xxxxxx

ARTICLE TYPE

Mechanically Stable Single-layer Mesoporous Silica Antireflective Coating on Solar Glass

Longqiang Ye,[a] Shuming Zhang,[a] Qing Wang,[a] Lianghong Yan,[b] Haibing Lv,[b*] and Bo Jiang[*a]

Received (in XXX, XXX) Xth XXXXXXXXX 20XX, Accepted Xth XXXXXXXXX 20XX

DOI: 10.1039/b000000x

A single-layer antireflective (SLAR) coating with extremely high photovoltaic transmittance (T_{PV}) at 400-1100 nm was designed with the aid of thin film design software (TFCalc^{TM}). The AR coating was prepared by evaporation-induced self-assembly using tetraethylorthosilicate (TEOS) as precursor and cetyltrimethylammonium bromide (CTAB) as template. The measured PV transmittance reaches as high as 98.7%, which is in good agreement with the theoretical value. Meanwhile this SLAR coating has excellent mechanical robustness, which passed the 3H pencil hardness test and abrasion test. This SLAR coating with high transmittance and good mechanical property will find important application in the field of solar cells.

Introduction

Solar glass, which is transparent to sunlight, serves as a window to protect solar cells from physical shock and corrosion.[1-2] Reflection from the glass for a normal angle of incidence can reach as high as ~8%. This is undesirable and detrimental to the light-to-electricity conversion efficiency in solar cells or any other types of optical devices that require minimal reflection. Therefore, achieving antireflection at the glass surface is significant to further enhance energy conversion in solar cells.

For an ideal homogeneous single-layer antireflective (SLAR) coating, zero reflection is achieved by fulfilling two requirements: first, the film thickness of the coating should be $\lambda/4$, where λ is the wavelength of the incident light; and second, the refractive index of the film should be equal to $(n_a n_s)^{1/2}$, where n_a and n_s are the refractive indices of air and substrate, respectively.[3] The first condition can be easily met, while the second requirement is more difficult. The refractive index of glass is about 1.52, which implies that the refractive index of antireflective (AR) coating must be about 1.22. Such a low refractive index is difficult to be realized with normal low-index material (the lowest refractive index is above 1.38 for MgF_2).[4] This conundrum is usually solved by introducing nanopores into the AR coating. In the past several decades, many approaches have been developed to prepare nanoporous AR coating. These methods include phase separation,[5-6] etching,[7-8] oblique-angle deposition,[9-10] layer-by-layer deposition method,[11-12] and sol–gel method.[13-14] Among these methods, the potential of sol–gel-derived AR coatings has been clearly shown because the sol–gel thin film process permits independent tailoring of both microstructure and chemical composition of the deposited films.[15]

Sol–gel-derived silica AR coating mainly includes base- and acid-catalyzed AR coating.[16] Base-catalyzed silica AR coating consists of a layer of silica particles, randomly stacked on the substrates' surface. The inter-particle and particles' interior porosity lowers the refractive index of coating to the square root of the refractive indices of glasses. This gives sol-gel silica AR coating with nearly 100% transmission.[17] However, the use of base-catalyzed sol–gel silica AR coatings is hindered by their susceptibility to mechanical robustness, especially in the field of solar glass. Since the solar glass in use is subjected to clean process, the AR coatings deposited on solar glass must have sufficient mechanical properties to avoid damage due to erosion and abrasion.[18] Acid-catalyzed silica AR coating is strongly cross-linked by chemical bond, the film intrinsic possesses strong mechanical strength. However, the coatings consisting of linear chains present dense structure, resulting in a high refractive index and hence low transmittance.[19] Base/acid two-step catalyzed sol–gel method and normal acid-catalyzed templating sol–gel process showed to be suitable routes to achieve AR coatings with improved mechanical properties.[20-23] Mesoporous silica films prepared by evaporation-induced self-assembly (similar to sol-gel method) have attracted considerable attention because of their potential use in the areas of sensors, photo-catalysis, low-*k* and medical application.[24]

In this paper, we fabricate mesoporous AR coatings by evaporation-induced self-assembly using cetyltrimethyl -ammonium bromide (CTAB) as template. CTAB is employed as a surfactant to form micelles so that the mesopores can be formed in the films after the subsequent decomposition of the micelles at high temperature. The obtained films exhibit not only extremely high transmittance but also excellent mechanical robustness. The maximum transmittance increased from 92.0% to 99.9% for glass substrate and the PV transmittance reached as high as 98.7%.

Experimental Section

Materials

Tetraethylorthoxylsilicane (TEOS) was purchased from Sigma-Aldrich. CTAB was purchased from Xiya Reagent. The water was deionized. Ethanol and hydrochloric acid (37%) were purchased from Kelong Chemical Reagents Factory (Chengdu, China). All chemicals were used without further purification.

Film Preparation

Precursor solutions were prepared by addition of cationic surfactant CTAB to polymeric silica sols made by a two-step process. The polymeric silica sol was prepared by refluxing an ethanolic solution containing TEOS, H_2O and diluted HCl (mole ratios: 1TEOS: 3.8EtOH: 1H_2O: 5×10-5HCl) at 60 ℃ for 1.5 h. A second solution was prepared with CTAB, EtOH, H_2O and HCl, and slowly added to the prehydrolyzed solution; the final molar ratios were TEOS: EtOH: H_2O: HCl: CTAB =1: 22: 5: 0.004: x. The CTAB/SiO_2 molar ratio x was varied from 0 to 0.20. The final sols were stirred for 2 h at 30 ℃ and aged for 48 h at room temperature in a closed vessel. The obtained sols were diluted with EtOH (1:1) and deposited on glass substrates by dip-coating in a humidity-controlled room at 30% RH. The final films were obtained by pre-heating in air at 100 ℃ for 1 h and then 400 ℃ for 2 h to completely remove the organic species.

Characterization

Theoretical transmittance spectrum of the homogeneous SLAR coating was calculated with TFCalcTM program (Software Spectra Inc), and the experimental transmittance spectrum was measured with an UV-vis spectrophotometer (Mapada, UV-3100PC). Surface morphologies and cross-sections of the AR coating were investigated separately by atomic force microscopy (AFM) (SEIKO SPA-400) and JSM-5900LV scanning electrons microscope (SEM). The refractive indices of AR coatings were determined by ellipsometry (SENTECH SE850 UV). The mechanical robustness of the resultant coatings was assessed in the abrasion test, in which the standard normal stress 25 kPa was applied with rotational shear (100 rpm for 0.5 h) on an abrasion-resistance machine (DZ-8103, Dongguan City Dazhong Instrument CO, LTD.). The mechanical damages were determined by the change of the transmittance before and after the abrasion test. Pencil hardness was measured by a pencil hardness tester (GB/T6739-1996).

Results and Discussion

Theoretical design and calculation

AR coatings can be designed using many methods, such as vector method, admittance loci, and so on. However, these methods involve much calculation, making them tedious and time-consuming. Computer-aided design is the preferred method because it is fast and straightforward. The theoretical SLAR coating described here was obtained with the aid of thin film design software TFCalcTM. The solar weighted average transmittance (PV transmittance, T_{PV}), which is the ratio of the usable photons transmitted to the total usable photons, was adopted to estimate quantitatively the effectiveness of the AR coating on the solar cell performance. The value of T_{PV} can be evaluated by normalizing the transmittance spectra with the solar spectral photon flux integrated over a wavelength range of 400-1100 nm (which is crucial for silicon solar cells).[25] The T_{PV} is given by

$$T_{PV} = \frac{\int_{400}^{1100} T_\lambda S_\lambda d_\lambda}{\int_{400}^{1100} S_\lambda d_\lambda} \quad (1)$$

Where T_λ is the wavelength-dependent transmittance of the coated glass, S_λ is the solar radiation function for air mass 1.5 (ASTM G173-03). Fig. 1 shows the PV transmittance as a function of the refractive index and film thickness of SLAR coating. The refractive index and thickness of SLAR coating were varied from 1.00 to 1.52 and 25 nm to 250 nm, respectively. As the refractive index was in the range of 1.19-1.26 and the thickness was in the range of 123-149 nm, high *TPV* values of approximately 98.5% could be achieved. The ideal SLAR coating with the highest T_{PV} of 98.7% for best light harvesting should have a refractive index of 1.22 and a thickness of 133 nm.

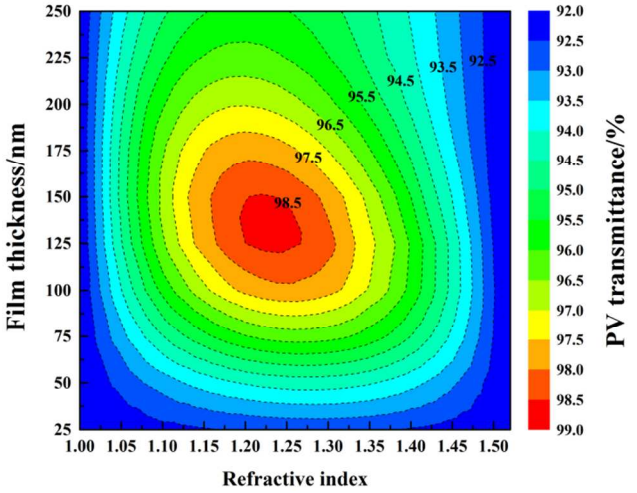

Figure 1. Contour plot of the PV transmittance as a function of refractive index and film thickness of the SLAR coating.

Refractive index

In order to obtain the highest PV transmittance, the refractive index of AR coating must be tuned to 1.22. Fig. 2 shows the change of refractive index of AR coatings as a function of CTAB/SiO_2 molar ratio. The refractive index initially increases with increasing CTAB concentration, reach a minimum of 1.18; then an decrease in value of refractive index is observed with further increase of CTAB content. According to the Lorentz–Lorenz equation,[26] refractive index of the coating is related to porosity. Higher porosity leads to lower refractive index, as shown in Fig. 2. The removal of CTAB by thermal decomposition increases the film porosity resulting in a lower refractive index of the film. When the ratio of CTAB/SiO_2 is greater than 0.16, a decrease in porosity was observed probably because the mesoporous walls become too thin to resist excessive condensation between silanol groups resulting in a partial collapse of the porous structure during calcination. The ratio of 0.12 was chosen as the optimum ratio for the fabrication of the

AR coating in this work.

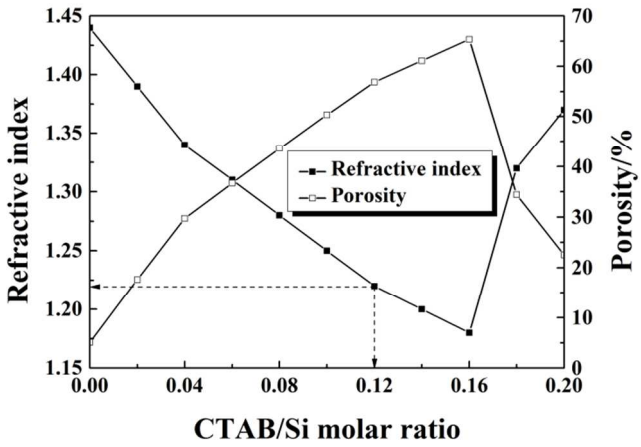

Figure 2. Change in refractive index and porosity of AR coatings as a function of CTAB/SiO2 starting ratio.

Optical property

A SLAR coating with a refractive index of 1.22 and a thickness of 133 nm was prepared in this work. The thichness can be easily controlled by varying the dip-coating speed and/or the sol concentration in the sol–gel process.[27] Fig. 3 shows the transmittance spectra of the coating before and after calcination. The maximum transmittance of uncalcined thin film reached 95.0%, similar to the dense acid-catalyzed silica coating.[16] After removal of CTAB, the transmittance increased greatly with a maximum transmittance of 99.9% at 650 nm. The porosity of the film is about 57% estimated on the basis of the value of refractive index. The measured T_{PV} in the region of 400-1100 nm is 98.7%, which is in good agreement with the theoretical result obtained by TFCalc™ program. The experimental transmittance fits well within the theoretically predicted one, indicating absence of diffusive reflection and uniformly distributed nanopores in the film. The cross-sectional structure of the nanoporous film was studied by SEM. From the cross-sectional image shown in Fig. 4a, it could be seem that the AR coating is uniform in thickness. AFM images (Fig. 4b) indicate that the film has a root-mean-square (RMS) roughness (Rq) of ~0.69, which is too small to cause any intense surface light scattering.

The smooth surface can be well explained by the formation mechanism of the mesoporous thin film by evaporation-induced self-assembly.[28] As shown in Fig. 5, a homogeneous solution of soluble silica and CTAB was prepared in ethanol/water solvent with $c_o << c_{mc}$, where c_o and c_{mc} are the initial and critical micelle concentration of CTAB, respectively. During dip-coating, the entrained solution experiences preferential evaporation of ethanol, progressively enriching the concentrations of water, HCl, and the nonvolatile CTAB and silica species. The rapid evaporation of the solvent allows the micellar organization and stabilization by gelation of a silica network. In other words, the silicate encases the well-ordered surfactant micelles, and there are hardly any CTAB templates on the surface of the coating. After subsequent removal of the micellar template by calcination, highly ordered mesostructure is formed and almost all the pores are located within the inner part of the coating. Therefore, the surface of the porous coating is smooth.

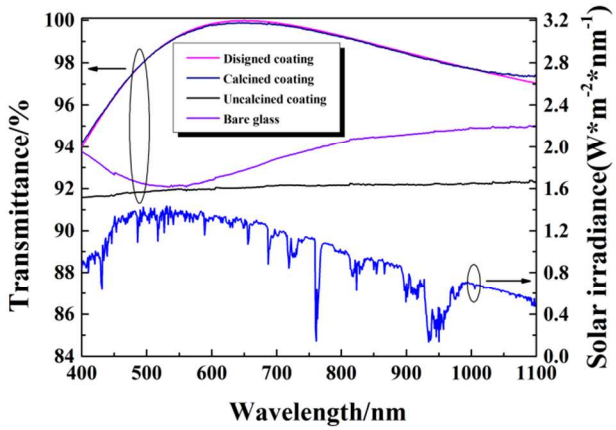

Figure 3. Designed and measured transmittance spectra of the SLAR coating, overlaid with the corresponding solar spectral irradiance at AM1.5 as a reference.

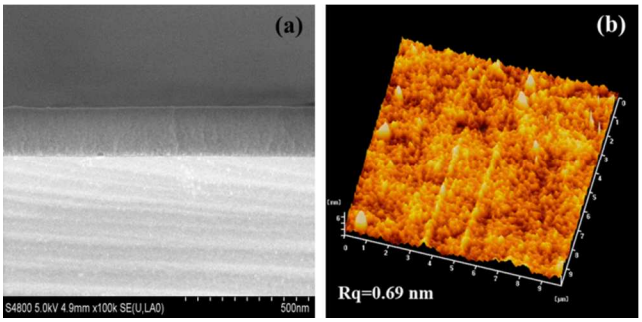

Figure 4. (a) Cross-sectional SEM and (b) AFM images of the AR coating.

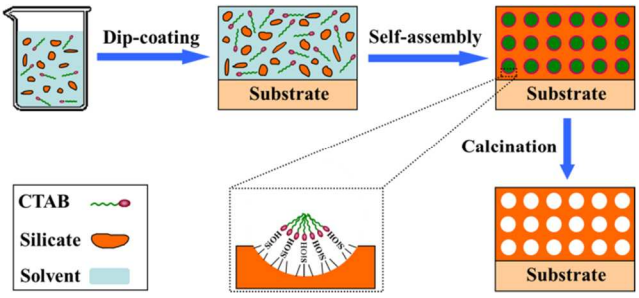

Figure 5. Schematic illustration of the formation mechanism of highly antireflective, mechanically robust SLAR coating.

Mechanical performance

For outdoors use, the mechanical robustness of the AR coatings is very important due to harsh atmospheric conditions and imperative cleaning processes. To assess the mechanical properties of the coatings, the hardness of the AR coatings was examined by the pencil hardness test. If the adhesion force between the thin film and the substrate was only Van der Waals interactions, it usually could not withstand 1B pencil hardness tests.[29] The pencil hardness of the calcined AR coatings was found to be 3H, indicating the presence of some covalent bonds. The hardness is good enough for normal use in solar energy application.[30] Abrasion-resistance is another important feature as films usually are subjected to washing process for removing the contaminants. The decrease of the PV transmittance was adopted to evaluate the abrasion-resistance of the AR coatings after abrasion test, which provide a technologically relevant

performance metric. As shown in Fig. 6, the AR performance of the coating remains almost unchanged after abrasion test, only 0.2% reduction in the region of 400-1100 nm was observed, showing an excellent abrasion-resistant property of this AR coating. The mechanical robustness can also be explained by the formation of mesoporous film. During the formation of films, CTAB micelles were encased by silica, and after removal the micelles, the mesopores were closed by network cross-linking silica structure.

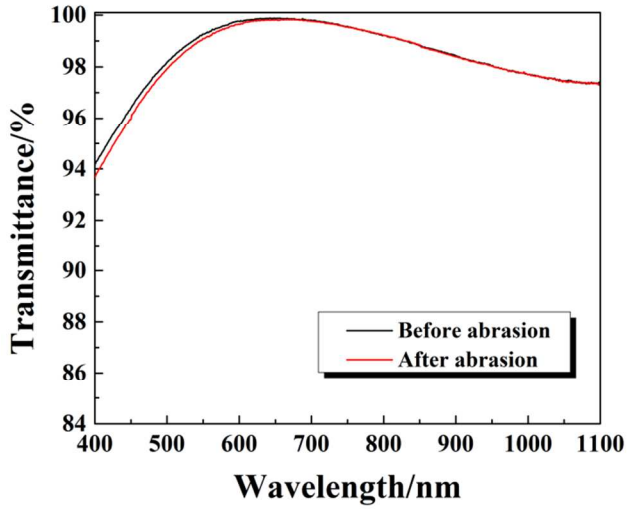

Figure 6. Change in transmittance of the AR coating before and after abrasion.

Conclusion

In summary, a single-layer antireflective coating with extremely high PV transmittance in the wavelength range of 400-1100 nm was designed by computer-aid calculation and the designed AR coating was prepared by evaporation-induced self-assembly. As a result, the maximum transmittance of the coated glass substrate reaches as high as 99.9% and the PV transmittance reaches a value of 98.7%, an increase of 6.7% as compared with the uncoated glass substrate, showing an excellent broadband AR effect from visible light to NIR wavelengths. Moreover, the AR coating has excellent mechanical robustness, which passed the 3H pencil hardness test and abrasion test. This film with high transmittance and excellent mechanical robustness can have potential applications in energy harvesting and optical instrumentation.

Acknowledge

The authors gratefully acknowledge the support from National Natural Science Foundation of China (J1103315).

Notes and references

[a]*Key Laboratory of Green Chemistry and Technology and College of Chemistry, Sichuan University, Chengdu, China, Tel.: +86 28 85418112; fax: +86 28 85412907 E-mail: jiangbo@scu.edu.cn*
[b] *D Research Center of Laser Fusion, China Academy of Engineering Physics, Mianyang, China E-mail: haibinglv@163.com*

† Electronic Supplementary Information (ESI) available: [details of any supplementary information available should be included here]. See DOI: 10.1039/b000000x/

1 V. Petrova-Koch, R. Hezel, A. Goetzberger, High-efficient low-cost photovoltaics: recent developments, Springer, 2009.
2 L. Q. Liu, X. L. Wang, M. Jing, S. G. Zhang, G. Y. Zhang, S. X. Dou, G. Wang, *Adv. Mater*, 2012, **24**, 6318-22.
3 H. A. Macleod, Thin-film optical filters, CRC Press, 2001.
4 H.K. Raut, S.S. Dinachali, K.K. Ansah-Antwi, V.A. Ganesh, S. Ramakrishna, *Nanotechnology*, 2013, **24**, 505201.
5 S. Walheim, E. Schäffer, J. Mlynek, U. Steiner, *Science*, 1999, **283**, 520-22.
6 X. Li, X. Yu, Y. Han, *J. Mater. Chem. C*, 2013, **1**, 2262-85.
7 L. Yao, J. He, *Langmuir*, 2013, **29**, 3089-96.
8 J. Xiong, S. N. Das, J. P. Kar, J. H. Choi, J. M. Myoung, *J. Mater. Chem. C*, 2010, **20**, 10246-52.
9 J. Q. Xi, J. K. Kim, E. F. Schubert, *Nano. Lett*, 2005, **5**, 1385-7.
10 J. Q. Xi, M.F. Schubert, J. K. Kim, E. F. Schubert, M. Chen, S. Y. Lin, W. Liu, J. A. Smart, *Nat. Photonics*, 2007, **1**, 176-9.
11 J. A. Hiller, J. D. Mendelsohn, M. F. Rubner, *Nat. Mater*, 2002, **1**, 59-63.
12 G. M. Nogueira, D. Banerjee, R. E. Cohen, M. F. Rubner, *Langmuir*, 2011, **27**, 7860-7867.
13 X. Zhang, B. Xia, H. Ye, Y. Zhang, L. Yan, H. Lv, B. Jiang, *J. Mater. Chem*, 2012, **22**, 13132-40.
14 X. Zhang, H. Ye, B. Xiao, L. Yan, H. Lv, B. Jiang, *J. Phys. Chem. C*, 2010, **114**, 19979-83.
15 A. L. Pénard, T. Gacoin, J. P. Boilot, *Acc. Chem. Res*, 2007, **40**, 895-902.
16 A. Vincent, S. Babu, E. Brinley, A. Karakoti, S. Deshpande, S. Seal, *J. Phys. Chem. C*, 2007, **111**, 8291-8.
17 W. Stöber, A. Fink, E. Bohn, *J. Colloid. Interf. Sci*, 1968, **26**, 62-9.
18 M. Bautista, A. Morales, *Sol. Energ. Mater. Sol. C*, 2003, **80**, 217-25.
19 L. Ye, Y. Zhang, X. Zhang, T. Hu, R. Ji, B. Ding, B. Jiang, *Sol. Energ. Mater. Sol. C*, 2013, **111**, 160-4.
20 H. Ye, X. Zhang, Y. Zhang, L. Ye, B. Xiao, H. Lv, B. Jiang, *Sol. Energ. Mater. Sol. C*, 2011, **95**, 2347-51.
21 F. Chi, L. Yan, H. Lv, B. Jiang, *Mater. Lett*, 2011, **65**, 1095-7.
22 K. Wongcharee, M. Brungs, R. Chaplin, Y. Hong, R. Pillar, E. Sizgek, *J. Sol-Gel. Sci. Techn*, 2002, **25**, 215-21.
23 G. San Vicente, R. Bayón, N. Germán, A. Morales, *Thin. Solid. Films*, 2009, **517**, 3157-60.
24 P. Innocenzi, L. Malfatti, *Chem. Soc. Rev*, 2013, **42**, 4198–216.
25 S. Chhajed, M. F. Schubert, J. K. Kim, E. F. Schubert, *Appl. Phys. Lett*, 2008, **93**, 251108-11.
26 B. E. Yoldas, D. P. Partlow, *Thin. Solid. Films*, 1985, **129**, 1-14.
27 D. Grosso, *J. Mater. Chem*, 2011, **21**, 17033-8.
28 D. Grosso, F. Cagnol, G. d. A. Soler-Illia, E. L. Crepaldi, H. Amenitsch, A. Brunet-Bruneau, A. Bourgeois, C. Sanchez, *Adv. Funct. Mater*, 2004, **14**, 309-22.
29 L. Xu, J. He, *J. Mater. Chem. C*, 2013, **1**, 4655-62.
30 B. T. Liu, W. D. Yeh, W. H. Wang, *J. Appl. Polymer Sci*, 2010, **118**, 1615-9.